FELIX: THE DUTCH FREE ELECTRON LASER FOR INFRARED EXPERIMENTS

P.W. van Amersfoort, R.W.B. Best, C.A.J. van der Geer,
W.J. Mastop, B.J.H. Meddens, A.F.G. van der Meer, D. Oepts,
and M.J. van der Wiel

FOM-Institute for Plasma Physics, Edisonbaan 14,
3439 MN Nieuwegein, The Netherlands

We review the status of the Dutch Free Electron Laser for Infrared eXperiments (FELIX), with which radiation in the range between 3 μm and 3 mm will be generated. Among our research objectives are (i) rapid tunability and (ii) mode reduction by means of an intracavity etalon. The first stage of the project deals with generation of radiation with a wavelength between 8 and 80 μm. The design of the accelerator, with which 70-A, 3-ps bunches are accelerated to a maximum energy of 45 MeV, is discussed. It consists of a triode, a 4-MeV buncher, and a travelling-wave linac.

Introduction

The FELIX project addresses the construction of a tunable Free Electron Laser in the infrared and microwave region [1]. Presently we are in the process of designing the accelerating system, which should deliver microbunches with a peak current of 70 A and a duration of 3 ps. This high current is needed to achieve a gain per pass of at least 0.2, which is required to overcome the losses occurring when an intracavity etalon is inserted. The latter will be done to reduce the number of active cavity modes, which makes it possible to make pulses with a narrow bandwidth and a high peak power available to external users. One out of every three rf-buckets of the linac will be filled in order to restrict the average beam current to 200 mA, and hence to keep beam loading within reasonable limits.

We intend to use the undulator of the former UK-FEL project [2] in Stage I of our project. This planar undulator consists of 4 sections, each containing 19 periods of REC magnets with a wavelength λ_u= 65 mm. The magnetic field on axis can be varied by adjusting the undulator gap width, the maximum value is B=4400 G.

Gain Considerations

The small-signal, single-pass (peak) gain G_o for an electromagnetic wave packet with central wavelength λ_s travelling through a planar undulator is usually calculated as

$$G_o = I/377\ \sqrt{(\lambda_s/\lambda_u)}\ N^2\ k_{rms}^2/(1+k_{rms}^2)^{3/2}\ \{J_0(\xi)-J_1(\xi)\}^2 \qquad (1)$$

where I denotes the peak current, N denotes the number of undulator periods, and k_{rms} denotes the undulator strength, $k_{rms} \approx B[kG]\lambda_u[cm]/15.2$. Further, J_0 and J_1 denote the Bessel functions of order zero and one, respectively, and $\xi=0.5\ k_{rms}^2/(1+k_{rms}^2)$. The highest gains are

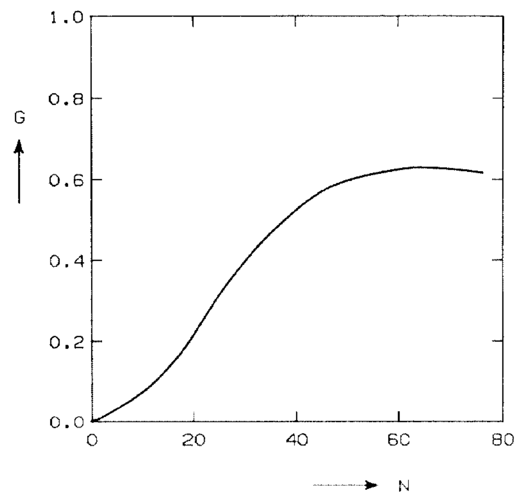

Fig. 1. The corrected gain as a function of the number of periods of the UK-FEL undulator, for a particle energy of 25 MeV.

expected for $k_{rms} \approx 1$, which for the UK-FEL undulator corresponds to a field strength B=2275 G. At this value, the wavelength region from 8 to 69 μm can be covered when the electron energy is varied from 15 to 45 MeV.

Eq. (1) is only valid for 'ideal', tenuous electron beams, i.e., for cw beams with negligible energy spread and emittance, and no space charge effects. Bizzarri *et al.* [3] discuss semi-analytic correction factors accounting for the longitudinal coupling of the wave with the microbunches, for the energy spread inside the electron beam, and for the finite beam emittance. In determining the number of undulator periods N, which is optimum for our application, it is worthwhile to note that the first two correction factors decrease strongly with increasing N. Thus, although G_o is proportional to N^2, the corrected gain, G, decreases with increasing N when short-pulse and energy-spread corrections dominate. This is illustrated in Fig. 1, where we show G versus N for λ_s=25 μm; the normalized beam emittance is taken equal to ε_n=50 π mm mrad, the energy spread is taken equal to σ_e=0.35 %, and the 'full-width-half-maximum' radius and semi-length of the bunches is taken equal to $\sigma_{x,y}$=0.5 and σ_z=0.4 mm, respectively. It is observed that G levels off at N=57. On the basis of this result, and of similar results for other wavelengths, we decided to use two sections (N=38) of the UK-FEL undulator in our project. This choice is based upon the following considerations: (i) the gain increases only modestly when N is further increased, (ii) saturation of the electromagnetic intensity is reached in a shorter time when the cavity length is shorter, and (iii) control of beam walk-off, as induced by field errors, is more difficult with increasing N.

In Fig. 2 we show G versus λ_s, for B=2275 G and N=38. The corresponding electron beam energy is given in the insert. G first increases with increasing λ_s, as predicted by Eq. (1), and decreases subsequently due to the reduced 'longitudinal filling'. Nevertheless, G is between 0.4 and 0.5 over the entire range from 8 μm to 69 μm. We also show results for B=1250 G and B=4400 G, which suggest that the wavelength region from 5 μm to 160 μm can be covered with

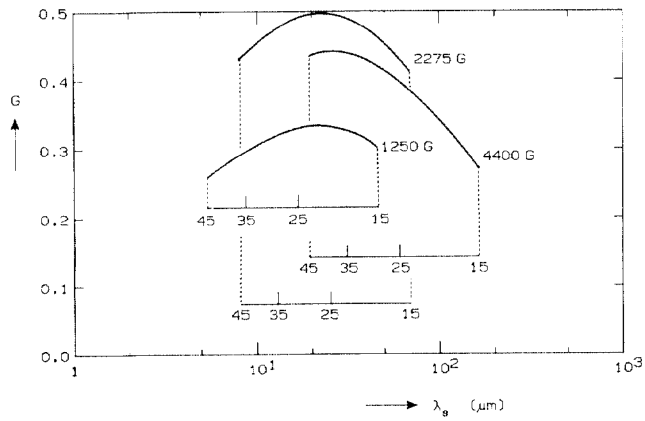

Fig. 2. The gain as a function of the wavelength of the FEL radiation.

the UK-FEL undulator at a gain between 0.25 and 0.5, provided that the desired beam quality can be maintained from 15 to 45 MeV.

We emphasize that collective effects, which can lead to a strong enhancement of the gain, are not taken into account here. In order to obtain a more accurate view of the amplification process, needed to make a final design of the optical cavity, numerical simulations have been initiated. Meanwhile, we choose to base the design of FELIX on conservative calculations as above.

The Electron Injector

A schematic view of the electron injector is shown in Fig. 3. The electron gun is a triode equipped with a grid, which is modulated at 1 GHz. The triode is capable of producing bunches with a charge of 200 pC and a duration of 250 ps, at an extraction voltage of 100 kV.

The bunching system consists of a 1-GHz subharmonic pre-buncher, a 3-GHz buncher, and (possibly) an energy selector. The buncher is of the $2\pi/3$-mode travelling-wave type and has a total length of 43 cm. Its exit energy is 4 MeV (at 20 MW input power). The buncher has been designed such, that the particle trajectories in ϕ-z-space do not intersect for a large range of input phases [4], so that

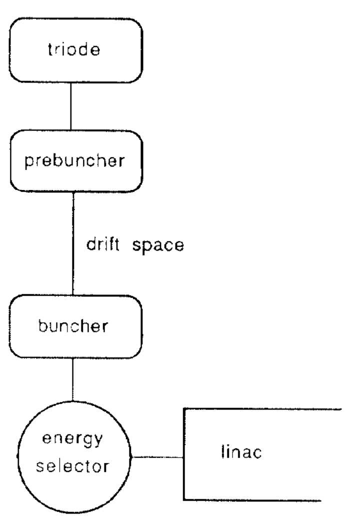

Fig. 3. Schematic view of the electron injector.

an unambiguous energy-phase relation can be maintained, which is essential for minimizing the energy spread in the succeeding accelerating section. The design philosophy is illustrated in Fig. 4, where we show the evolution of the input phase. Phases between -60° and 40° are seen to be 'compressed' without intersections.

PARMELA simulations of the *pre*bunching process show that, at a prebuncher peak voltage of 40 kV, 360°-bunches with a charge of 220 pC are compressed to roughly 100° after passing through a drift space of 17 cm, whereas some 50 % of the total charge is within an interval of a few degrees. At a field strength of 12 MV/m in the buncher, they are further compressed to 6°, while a distinct energy-phase relation is maintained. The concomittant energy spread is of the order of +/- 250 keV.

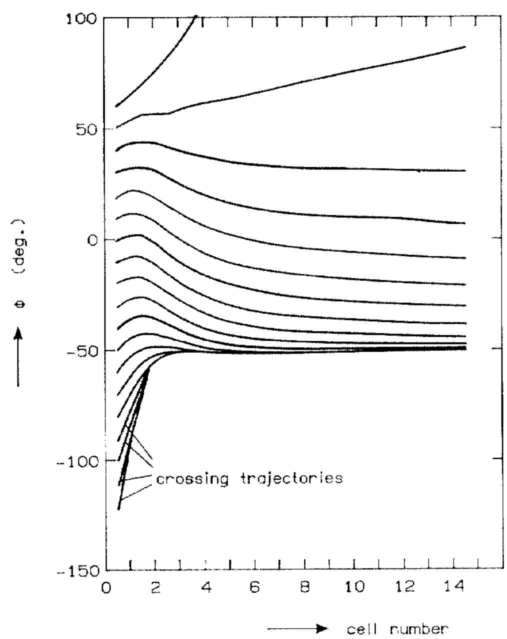

Fig. 4. Evolution of the particle phase through the buncher. Degrees refer to a frequency of 3 GHz ($360^\circ \propto 333$ ps). Particles at negative phases are ahead of the wave crest. Maximum acceleration is at 0°.

The Accelerating Section

A schematic view of the accelerating system is shown in Fig. 5. Two identical constant-gradient accelerating structures with the following characteristic properties are used: $2\pi/3$-mode, L=2.4 m, τ=0.44, r=60.6 MΩ/m, Q=12000. The corresponding relation between the attainable energy gain per structure, T, rf input power, P_o, and average beam current, i, is as follows:

$$T[\mathrm{MeV}] = 9.23\,\sqrt{P_o[\mathrm{MW}]} - 27.4\, i[\mathrm{A}] \tag{2}$$

Numerical calculations of the obtainable energy spread inside the bunch were done as follows. The linac is divided into a large number of cells with length dz, and the particle velocity, the particle phase with respect to the rf wave, the bunch length, and the electric field are assumed to be a constant in each cell. In the cell at position z, the energy gain of the electron at the center of the bunch is determined from $dT/dz=E_o\cos(\phi)-E_b$, where E_o and E_b denote the no-load field and the beam-induced field *in situ*, respectively. The phase shift is straightforwardly determined from the difference in velocity of the electrons and the wave. The energy gain and phase shift of the electrons at the edges of the bunch are determined in a similar way, where we take into account that the electron at the leading edge feels an extra accelerating field E_s, whereas the particle at the trailing edge feels a decelerating field E_s, due to the space charge in the bunch. This procedure gives the energies and phases at the exit of the cell in question, which serve as input parameters for the next cell. This way, we are able to determine the energy spread and bunch length as a function of z, at a constant klystron voltage V_k and beam current i. The influence of a variation of V_k or i is determined by repeating this procedure with a slightly different input phase, rf power, and beam current. This gives the energy spread, σ_e, as observed during the macropulse, i.e., averaged over many microbunches.

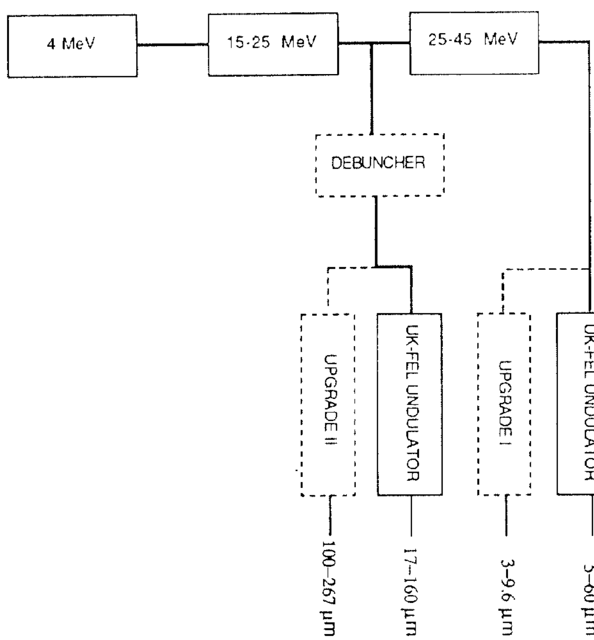

Fig. 5. Basic layout of FELIX. Upgrades to be established in Stage II are shown dashed.

Some results are presented in Table 1. Each row in this table contains two lines, showing for each of the two sections the input power, P_o, injection phase, Φ, exit bunch length, $\delta\Phi_{out}$, exit energy, T_{out}, and the energy spread, σ_e. The bunch length at injection is taken equal to 6^o and the injection energy is taken equal to 4 MeV +/- 250 keV, where it is assumed that the particle at the leading edge has the smallest energy. Further, the variations of the klystron voltage and of the beam current are taken equal to +/- 0.1 % and +/- 0.5 %, respectively.

It is seen that the bunch length at the exit of the accelerator is reduced with respect to the value at the entrance, due to bunching in the low-energy part of the first structure. Further, the energy spread amounts to $\sigma_e \approx 0.3$-0.4 % in the entire energy range from 15 to 45 MeV, where we remark that our intention is to produce energies below 25 MeV with a single section. These values are consistent with assumptions made in estimating the gain.

Two sections of the UK-FEL undulator will be placed behind the second accelerating structure, see Fig. 5. This undulator covers the wavelength range from 5 to 60 µm. Two other sections are placed behind the first structure, covering the wavelength range from 17 to 160 µm. In case our short microbunch length inhibits operation at these long wavelengths, a debuncher will be installed in Stage II of the FELIX project. With two new undulators, to be installed in Stage II, the wavelength range can be upgraded to 3-267 µm. A further shift upwards to 3 mm will be realized with a separate VandeGraaff accelerator.

Table 1. Longitudinal particle dynamics.

P_o [MW]	Φ [°]	$\delta\Phi_{out}$ [°]	T_{out} [MeV]	σ_e [%]
8.0	-10	4.8	25	0.3
8.0	-3	4.8	46	0.3
3.0	-20	4.3	15	0.4
3.0	-10	4.3	25	0.6

Acknowledgements

This work was performed as part of the research program of the association agreement between the 'Stichting voor Fundamenteel Onderzoek der Materie' (FOM) and EURATOM, with financial support from the 'Nederlandse Organisatie voor Wetenschappelijk Onderzoek' (NWO) and EURATOM.

References

1. P.W. van Amersfoort *et al.*, Rijnhuizen Rept. RR88/176.
2. C.R. Pidgeon *et al.*, Nucl. Instr. Meth. A **259** (1987) 31.
3. U. Bizzarri *et al.*, ENEA Rept. RT/TIB/85/49.
4. G. Saxon, 1988. Private communication.